Acta virol. **27** : 299—310, 1983

STRUCTURAL ANALYSIS OF RNA SUBUNITS FROM AVIAN MYELOBLASTOSIS VIRUS (AMV)

J. KORB, J. ŠTOKROVÁ, J. ŘÍMAN

Institute of Molecular Genetics, Czechoslovak Academy of Sciences,
166 37 Prague, Czechoslovakia

Received July 16, 1982

Summary. — Subgenomic fragments were released from purified 35S AMV RNA using strongly denaturing conditions of 78% formamide and 3.9 M urea at 53 °C. The fragments were characterized by sedimentation and electron microscopic analysis. The presence of five distinct, reproducible size classes of RNA molecules with mean lengths 1.79 ± 0.07 μm, 1.36 ± 0.09 μm, 1.03 ± 0.09 μm, 0.7 ± 0.08 μm, and 0.42 ± 0.09 μm were demonstrated. Analysis of poly(A)$^+$ and poly(A)$^-$ RNA fragments revealed that splitting of 35S AMV RNA by strongly denaturing agents is not entirely random. Only one main distinct site of preferential splitting of the AMV RNA was located at 1.8 kb from the 3′ end of the genome. The other three sites located at 3.2 kb, 4.5 kb, and 5.9 kb from the 3′ end were much less distinct and were masked by random degradation of the molecules. The amount of poly(A)$^-$ RNA fragments of preferential lengths was increased by additional splitting of RNA molecules at preferential sites. No proteosynthetic activity was detected when subunits obtained by strong denaturation of 35S AMV RNA were analysed in a cell-free protein synthesis system.

Key words: AMV RNA; retrovirus RNA subunits; electron microscopy of RNA

Introduction

The genome of most of the retroviruses represents a single-stranded RNA which sediments at 60—70S in native state. This RNA can be dissociated by denaturation into subunits sedimenting at 30—40S (Duesberg, 1968; Erikson, 1969).

When purified 35S RNA was analysed by electron microscopy, a large number of molecules of intermediate size have been observed. The length distribution profile revealed the presence of RNA molecules ranging from 0.3 to 2.0 μm (Heine *et al.*, 1975). It has been suggested that this RNA represents fractions of the viral genome resulting from strong denaturation, i.e. conditions in which some hidden breaks in the retrovirus RNA can be revealed (Chi and Bassel, 1975). The integrity of the viral genome may be dependent on the conditions of both RNA isolation (Scheele and Hanafusa, 1972, Chen *et al.*, 1980) and virus maturation (Stoltzfus and Snyder, 1975; Štokrová *et al.*, 1982). However, statistical analysis of the length distribution profile of 35S AMV RNA has indicated that molecules of intermediate sizes fall into five distinct, reproducible size groups. This observation based solely on electron microscopy excludes the assumption of random degradation and suggests the existence of preferential degradation at specific sites located along the RNA molecules (Heine *et al.*, 1975). Such an enzymatic or mechanic degradation might take place preferentially at single-stranded exposed regions of highly organized structure.

The described results prompted us to carry out a more detailed electron microscopic and sedimentation characterization of 35S AMV RNA splitting and the topographic definition of the sites at which preferential degradation of RNA might take place. The RNA fragments were analysed for their proteosynthetic activity.

Materials and Methods

Virus. BAI strain A avian myeloblastosis virus was used in all experiments. The virus was purified from the blood of leukaemic chickens (Leghorn White) exsanguinated in terminal stages of myeloblastic leukaemia (Trávníček and Říman, 1973) or from virus-producing cultures of leukaemic myeloblasts grown in suspension (Říman and Beaudreau, 1970). Virus was concentrated by centrifugation in a discontinuous sucrose gradient of 5 ml of a 43% sucrose and 6 ml of a 23% sucrose made in 0.1 mol/l NaCl and 0.05 mol/l Tris-HCl pH 7.5 (TN buffer pH 7.5). The virus concentrated at the surface of the 43% sucrose layer was collected, diluted to about 12% sucrose and purified by centrifugation through 10 ml of a 23% sucrose made in TN buffer (pH 7.5). Both centrifugations were carried out in a Spinco SW25.2 rotor at 25,000 rev/min for 90 min at 4 °C.

RNA extraction. Total AMV RNA was extracted with phenol-sodium dodecyl sulphate (SDS) (Spiegelmann et al., 1970) or as described by Hayward (1977). RNA was fractionated on linear 10—30% sucrose gradients made in 0.1 mol/l NaCl, 0.05 mol/l Tris-HCl, pH 8.5 (TN buffer pH 8.5) and 0.1% SDS by centrifugation in a Spinco SW41 rotor at 38,000 rev/min for 120 min at 15 °C. The 60-70S RNA peak fractions were pooled and RNA was precipitated with ethanol. For the preparation of 35S RNA, the 60-70S RNA was dissolved in TN buffer pH 8.5 and heated at 90 °C for 1 min or alternatively denatured with formamide-urea (78% formamide, 3.9 M urea, 53 °C for 30 sec). The samples were cooled rapidly on ice and layered onto 10—30% sucrose gradients made in TN buffer pH 8.5 with 0.1% SDS and centrifuged in a Spinco SW41 rotor at 38,000 rev/min for 300 min at 15 °C. The 35S RNA peak fractions were pooled and precipitated with ethanol.

Sedimentation analysis. The 35S RNA was treated with the 78% formamide-3.9 mol/l urea mixture at 53 °C for 35 sec, cooled on ice and diluted with TN buffer (pH 8.5) or briefly dialyzed against this buffer. The solution (0.5 ml) was layered on top of linear 10—30% sucrose gradient supplemented with 0.1 mol/l NaCl. 0.01 mol/l Tris pH 7.2 (non-denaturing conditions), or 0.001 mol/l Tris pH 7.2 and 0.0002 mol/l EDTA (gently denaturing conditions), or 0.1 mol/l glyoxal in 0.01 mol/l phosphate buffer pH 7.2 (denaturing conditions) (Kung *et al.*, 1975). After centrifugation in a Spinco SW41 rotor at 38,000 rev/min for 300 min (or 550 min if a denaturing gradient was used), the fractions were collected and examined for absorbance or for radioactivity. The labelled 28S and 18S ribosomal RNAs were used as standards.

Separation of poly(A)$^+$ and poly(A)$^-$ strands of 35S RNA. 35S AMV RNA was treated with a mixture of 78% formamide — 3.9 mol/l urea at 53 °C for 35 sec, cooled on ice and dialyzed against TN buffer at 4 °C for about 20 min. The RNA was diluted and applied to an oligo(dT)-cellulose column as described by Spector *et al.* (1978). The fractions corresponding to poly(A)$^+$ and poly(A)$^-$ were collected and concentrated by ethanol precipitation.

Electron microscopy. RNA dissolved in TN buffer (pH 8.5) was spread by the protein monolayer technique (Kleinschmidt and Zahn, 1959) modified for strongly denaturing conditions (Robberson *et al.*, 1971). One microliter of RNA (20 μg/ml in TN buffer pH 8.5) was mixed with 100 μl fo

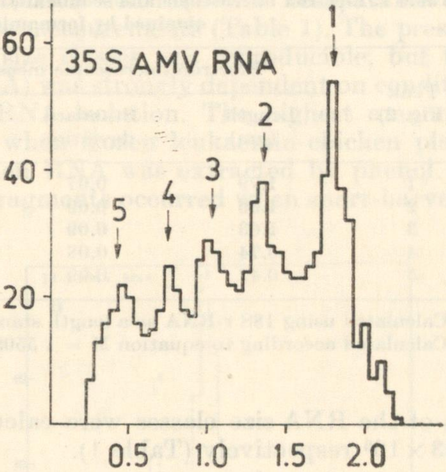

Fig. 2.
Length distribution profile of 35S AMV RNA
Abscissa: length in μm;
ordinate: number of molecules.
Description of the peaks in Table 1.

3.9 mol/l urea (Schwarz/Mann ultrapure) in 78% formamide (MCB), heated at 53 °C for 35 sec, quenched in ice-cold water. Two microliters of cytochrome c (Calbiochem, twice crystallized — 1.5 mg/ml in 1.5 mol/l Tris-HCl pH 8.5, 50 mmol/l EDTA) were added, and 50 μl of the mixture were spread onto a hypophase of deionized water (Korb *et al.*, 1981). The protein-RNA film was picked up on parlodion-coated grids, stained with uranyl acetate (Davis *et al.*, 1971), dehydrated in ethanol and rotary-shadowed with platinum-palladium alloy (80 : 20) ar an angle of 7°. Micrographs were taken with a JEM 100B electron microscope at an accelerating voltage of 60 kV. The magnification was calibrated with a diffraction grating carbon replica (Balzers). Molecule lengths were measured on prints at a total enlargement of 50,000 with a Hewlett-Packard 9864A digitizer and a 9830 HP calculator unit. ∅X174 DNA added to the RNA before spreading was taken as an internal length standard. The molecular weight of RNA was calculated using 18S rRNA of known molecular weight (Korb and Heine, 1978).

Gel electrophoresis. Electrophoretic analysis of RNA was performed in composite agarose-polyacrylamide gels as previously described (Korb *et al.*, 1976).

Results

Electron microscopic analysis of 35S AMV RNA

The 35S AMV RNA obtained by heat or formamide-urea denaturation of 60—70S RNA and purified on 10—30% sucrose gradients was denatured under strongly denaturing conditions (78% formamide and 3.9 M urea) and spread on top of deionized water (Korb and Heine, 1978). The length distribution profile of this RNA revealed the presence of smooth, stretched molecules ranging from 0.3 to 2.2 μm in length (Fig. 1). The molecules were characterized by the presence of five distinct, reproducible size classes with mean lengths of 1.79 ± 0.07 μm, 1.36 ± 0.09 μm, 1.03 ± 0.09 μm, 0.74 ± 0.08 μm and 0.42 ± 0.09 μm, respectively (Fig. 2). The position of these size classes of molecules was identical in different RNA preparations, but their proportion varied, depending on the type of virus propagation and RNA isolation. Using 18S rRNA as a standard (mol. wt. = 0.7 megadaltons) the

Table 1. Electron microscopic and sedimentation characteristics of 35S AMV RNA subunits obtained by formamide-urea denaturation

Peak (Fig. 2)	Electron microscopic measurement			Sedimentation analysis	
	Length (μm)	Standard deviation	M_r ($\times$ 10^6)*	S value	M_r ($\times$ 10^6)**
1	1.79	0.07	2.70	35	2.71
2	1.36	0.09	2.05	32	2.24
3	1.03	0.09	1.56	28	1.69
4	0.74	0.08	1.12	24	1.23
5	0.42	0.09	0.63	18	0.67

* Calculated using 18S r-RNA as a length standard (Korb and Heine, 1978).
* Calculated according to equation $M = 1\,550S^{2.1}$ (Spirin, 1963).

M_r of the RNA size classes were calculated to be 2.70, 2.05, 1.56, 1.12, and 0.63×10^6 respectively (Table 1).

Sedimentation analysis

The presence of molecules of intermediate size was confirmed by sedimentation and electrophoretic analysis. 35S AMV RNA was denatured by the formamide-urea method and analysed by sedimentation analysis in strongly denaturing (glyoxal), moderately denaturing (low salt) and non-denaturing (high salt) sucrose gradients. The sedimentation profile of denatured 35S AMV RNA analysed in the denaturing sucrose gradient is shown in Fig. 3. Five peaks or shoulders corresponding to the sedimentation constants 35S, 32S, 28S, 24S, and 18S are present. Similar profiles were observed when sedimentation analysis was performed under gently denaturing conditions or non-denaturing conditions (data not shown). Molecular weight of RNA

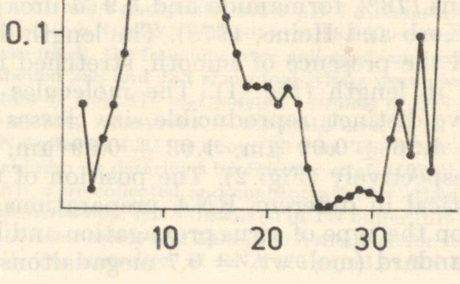

Fig. 3.
Sedimentation profile of denatured 35S AMV RNA analysed in the denaturing sucrose gradient (0.1 mol/l glyoxal)
Abscissa: number of fractions; ordinate: absorbance (A_{260})

calculated from the stated sedimentation constant was comparable with that obtained by electron microscopic measurements (Table 1). The presence and size of molecules of individual size classes was reproducible, but their proportion (percent of intact 35S RNA) was strongly dependent on conditions of cultivation and the method of RNA isolation. The highest amount of subgenomic fragments was present when frozen leukaemic chicken plasma was used for virus isolation and when RNA was extracted by phenol. The lowest amount (about twice) of the fragments occurred when short-harvested

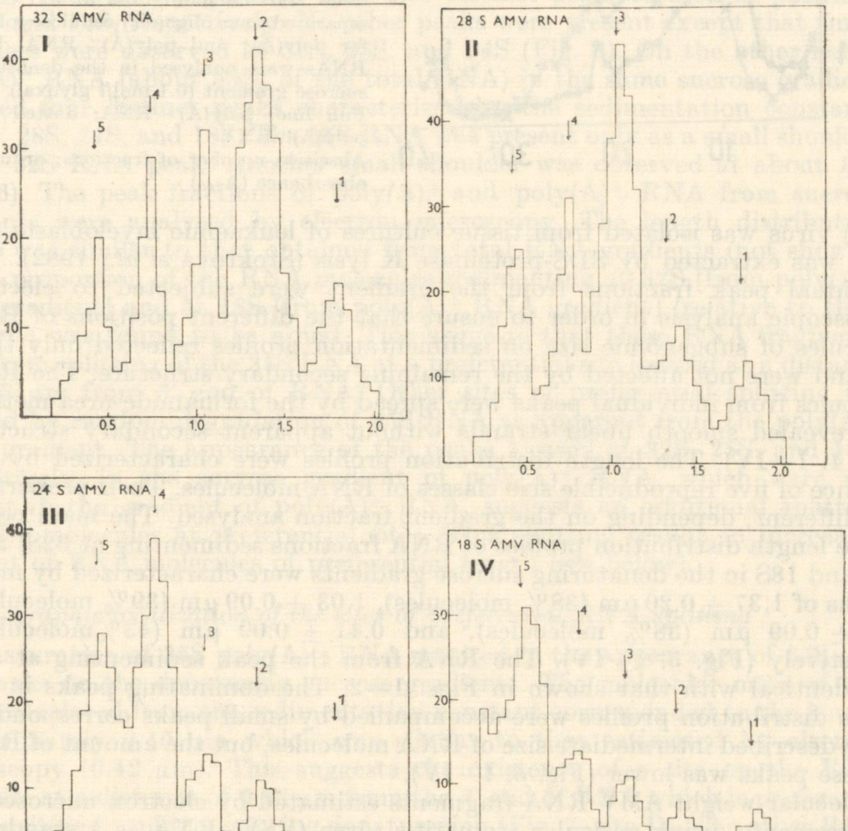

Fig. 5.

Length distribution profile of 35S AMV RNA fragments separated in the denaturing sucrose gradient (0.1 mol/l glyoxal)

The peak fractions were examined in the electron microscope.

I — fraction sedimenting at 32S; II — fraction sedimenting at 28S; III — fraction sedimenting at 24S; IV — fraction sedimenting at 18S.

Abscissa: length in μm; ordinate: number of molecules.

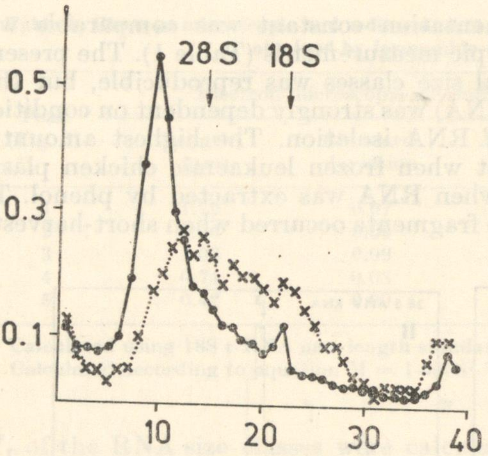

Fig. 6.
Sedimentation profile of 35S denatured AMV RNA

AMV RNA was denatured by 78% formamide and 3.9 mol/l urea at 53 °C and separated on an oligo(dT)-cellulose column for poly(A)$^+$ and poly(A)$^-$ RNA. Both RNAs were analysed in the denaturing sucrose gradient (0.1 mol/l glyoxal)
Full line: poly(A)$^+$ RNA; dotted line: poly(A)$^-$ RNA
Abscissa: number of fractions; ordinate: absorbance (A_{260})

(6 hr) virus was isolated from tissue cultures of leukaemic myeloblasts and RNA was extracted by SDS-proteinase K lysis (Štokrová *et al.*, 1982). The individual peak fractions from the gradient were subjected to electron microscopic analysis in order to ensure that the different positions of RNA molecules of subgenomic size on sedimentation profiles reflected only their size and were not affected by the remaining secondary structure. The RNA molecules from individual peaks were spread by the formamide-urea method and revealed smooth linear strands without apparent secondary structure (Fig. 4. I—IV). The length distribution profiles were characterized by the presence of five reproducible size classes of RNA molecules. Their proportion was different, depending on the gradient fraction analysed. The main peaks on the length distribution profiles of RNA fractions sedimenting at 32S, 28S, 24S, and 18S in the denaturing sucrose gradients were characterized by mean lengths of 1.37 ± 0.20 μm (38% molecules), 1.03 ± 0.09 μm (39% molecules), 0.74 ± 0.09 μm (38% molecules), and 0.41 ± 0.09 μm (43% molecules), respectively (Fig. 5. I—IV). The RNA from the peak sedimenting at 35S was identical with that shown in Figs. 1—2. The dominating peaks in the length distribution profiles were accompanied by small peaks corresponding to the described intermediate size of RNA molecules, but the amount of RNA in these peaks was lower (Fig. 5. I—IV).

Molecular weight AMV RNA fragments estimated by electron microscopy measurements, using vesicular stomatitis virus (VSV) RNA as a standard, was in good agreement with that determined from sedimentation constants (according to Spirin, 1963) (Table 1).

The results obtained by sedimentation analysis were also confirmed by gel electrophoresis of ^{32}P-labelled AMV RNA (data not shown).

Separation of poly(A)$^+$ and poly(A)$^-$ strands

AMV RNA was separated on an oligo(dT)-cellulose column to poly(A)$^+$ and poly(A)$^-$ RNA fragments which were then analysed in the denaturing

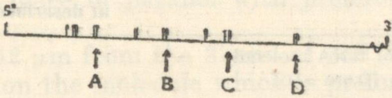

Fig. 7.
Topographic localization of sites of preferential splitting on the 35S AMV RNA
Arrows A, B, C, D represent the sites of preferential splitting obtained from electron microscopic analysis. The bars indicate the RNA fragments arising by additional splitting of RNA at multiple splitting sites.

sucrose gradients. Poly(A)+ RNA which represented about 45% of the total RNA revealed in the gradient only two distinct peaks located at positions of 35S and 18S, respectively. No other peaks were present except that small shoulders were observed at 32S, 28S, and 24S (Fig. 6). On the other hand, poly(A)$^-$ RNA (about 55% of the total RNA) in the same sucrose gradient revealed four distinct peaks characterized by the sedimentation constants of 32S, 28S, 24S, and 18S. The 35S RNA was present only as a small shoulder in the 32S RNA peak. Another small shoulder was observed at about 10S (Fig. 6). The peak fractions of poly(A)$^+$ and poly(A)$^-$ RNA from sucrose gradients were analysed by electron microscopy. The length distribution profile was similar to that obtained from total RNA gradients (not shown).

The proportion of the RNA molecules sedimenting at 32S [from poly(A)$^-$ RNA gradient] and at 18S [from poly(A)$^+$ RNA gradient] (relative to their mol. wt.) was found to be equal. This suggests that these RNA fragments arise from splitting of the 35S RNA at a preferential site located at a distance of 1.03 μm from 5′ end of RNA. Other sites of preferential splitting are masked by random degradation of 35S RNA as apparent from the poly(A)$^+$ RNA gradient. The appearance of the peaks located at 32S, 28S, and 18S, respectively, in the sucrose gradient of poly(A)$^-$ RNA, which were not present in the gradient of poly(A)$^+$ RNA, suggests an additional splitting of RNA molecules at preferential sites. This splitting results in increasing amount of RNA molecules of preferential length (see below).

Topographic localization of the sites of preferential RNA splitting

Denaturation of 35S poly(A)$^+$ RNA resulted in the appearance of 35S and 18S peaks on the denaturing sucrose gradients. The molecular mass of 18S RNA calculated from the sedimentation constant corresponded to the length approximately 0.40 μm which was similar to that estimated by electron microscopy (0.42 μm). This suggests the existence of a site on the RNA molecule at a distance of 0.42 μm from the 3′ end of RNA which is preferentially sensitive to splitting during denaturation (Fig. 7, site D). The other RNA molecular size classes corresponding to contour lengths of 0.74 μm, 1.03 μm, and 1.32 μm are produced by splitting of RNA at sites of preferential splitting (C, B, A) located at distances of 0.74 μm, 1.03 μm, and 1.32 μm from the 3′ end of RNA (Fig. 7). The production of molecules by splitting the genome at described positions were suggested by sedimentation analysis of denatured poly(A)$^+$ RNA, where small shoulders were observed at positions corresponding to the described lengths. However, the preference for splitting at sites A, B, C is much less distinct than at the site D.

Table 2. Possible RNA subunits obtained by splitting of 35S RNA molecule at described preferential sites

Part of RNA molecule (from – to)	Length of subunit (μm)	S^{20}_{w} interval
D – 3′ end	0.42	
C – D	0.32	
B – C	0.29	16 – 18S
A – B	0.33	
5′ end – A	0.43	
C – 3′ end	0.74	
B – D	0.71	21 – 24S
A – C	0.62	
5′ end – B	0.76	
B – 3′ end	1.03	
A – D	0.94	26 – 28S
5′ end – C	1.05	
A – 3′ end	1.36	32S
5′ end – D	1.37	

The existence of the molecules of preferential length was apparent not only from the length distribution profile of the 35S AMV RNA visualized under strongly denaturing conditions where the distinct size groups of molecules were observed, but also from the sedimentation profile of poly(A)$^-$ RNA fragments. Poly(A)$^-$ RNA fragment can arise not only from a direct splitting of the full length 35S RNA molecule at four preferential sites described above, but also by an additional splitting of different RNA fragments, which were not completely split at these sites. These RNA fragments constitute the population of molecules the sizes of which fall approximately in the size classes determined by direct spliting of the 35S RNA at preferential sites (Table 2). This results in the amplification of preferential size groups of poly(A)$^-$ RNA molecules.

The peak corresponding to the 32S poly(A)$^-$ RNA can be represented by molecules arising by splitting at site A [A to the 3′ end, on the molecules not containing poly(A)], as well as at site D (5′ end to D). The length of the two types of molecules is 1.33 μm and 1.35 μm, respectively. Similarly, the peak of the 28S poly(A)$^-$ RNA can be formed by molecules arising by splitting at sites A and D, B (B to the 3′ end, on the molecules not containing poly(A)] and site C (5′ end to C). The peak of the 24S poly(A)$^-$ RNA can contain molecules formed by splitting at sites A and C, B and D, C [C to the 3′ end, on the molecules not containing poly(A)] and site B (5′ end to B). Finally, the fraction of 18S poly(A)$^-$ RNA can be formed by molecules arising from preferential splitting at sites B and C, A and B, C and D, D [D to the 3′ end, on the molecules not containing poly (A)] and site A (5′ end to A) (Table 2). This amplification of the amount of molecules of preferential length is probably responsible for the appearence of distinct peaks on the sucrose gradient of poly(A)$^-$ RNA, whereas in the case of poly(A)$^+$ RNA these peaks were masked by random degradation taking place in parallel with preferential splitting.

The site D located at a distance of 0.42 μm from the 3′ end of 35S AMV RNA therefore represents the main site on the molecule which is preferen-, tially sensitive to spliting. The other sites A, B, and C located at 1.36 μm, 1.03 μm, and 0.74 μm, respectively, from the 3′ end of the RNA molecule also reveal preferential sensitivity to a disruption of the RNA molecule, but this preference is much less distinct than in the case of site D.

The described poly(A)$^+$ and poly(A)$^-$ subuunits released by strong denaturation of the 35S AMV RNA were analysed for their proteosynthetic activity in a cell-free protein synthesis system (Malý *et al.*, 1980). No proteosynthetic activity was detected when subunits sedimenting at 32S, 28S, 24S, and 18S were analysed.

Discussion

Electron microscopic analysis of the 35S AMV RNA preparations revealed a surprisingly large number of molecules of different sizes — all of them smaller than the 35S subunits (Heine *et al.*, 1975; Štokrová and Korb, 1977). These molecules represent fraction of the viral genome and may result from a process of degradation. However, results based on a statistical analysis of electron microscopic preparation indicate that the molecules fall into five distinct, reproducible size classes, an observation that excludes the assumption of random degradation (Heine *et al.*, 1975).

The presence of nucleases inside the virions is well known (Trávníček and Říman, 1966) and the nicking could take place at single-stranded regions of the genome which is characterized by high helicity (Cavalieri, 1974) However, since the release of subgenomic fragments of preferential length was observed on the already denatured 35S AMV RNA (during 35S RNA preparation), it is problematic to admit surviving of the complexes containing single-strand breaks and their disruption during the subsequent denaturation. The fragments were obtained regardless of the strength of previous denaturation of 60—70S RNA during preparation of 35S RNA subunits. Therefore, an additional hydrolysis of the originally intact 35S RNA genome takes apparently place during sample preparation.

Our results based on electron microscopy, sedimentation and electrophoretic analysis confirm the electron microscopic data of Heine *et al.* (1975) on non-random degradation of genomic RNA and suggest the existence of four sites on the genome where preferential splitting takes place. However, we have found substantial difference in the sensitivity of these sites to splitting. Only one main site with high preference for splitting has been found on the genome of 35S AMV RNA. This site is located at 1.8 kb from the 3′ end and the occuring fragments, 1.8 kb poly(A)$^+$ RNA and 5.9 kb poly(A)$^-$ RNA, are released in equimolar proportion. Recently Gonda *et al.* (1981) have identified only two RNA species, which were present in AMV virions and in AMV-transformed cells. The larger (7.2) kb species in presumably the genome of AMV and the smaller (2.3 kb) one may be a subgenomic messenger RNA that mediates oncogenesis by AMV. Moreover, the 2.3 kb species is present in significant amounts in the 70S RNA complex, and thus in this respect resembles a viral genome (Gonda *et al.*, 1981).

Distinct poly(A)$^+$ RNA fragment of 1.8 kb formed by splitting at the main preferential site is about 500 kb shorter than subgenomic messenger RNA described by Gonda *et al.* (1981). The observed site of preferential splitting could reflect some structural feature of the genome, being in some relation to the transcription of messenger RNA. The other three sites of preferential splitting at positions 3.2 kb, 4.5 kb, and 5.9 kb from the 3′ end are undoubtedly present on the AMV RNA as resulted from electron microscopy of the poly(A)$^+$ 32S, 28S, and 24S RNA fractions. Their significance is, however, much less in comparison with the 1.8 kb site. The occuring molecules of preferential length are here partially masked by random degradation of RNA.

Whereas the size of the released subunits was identical in different RNA preparations, their proportion was different depending on the type of virus propagation and RNA isolation. This difference can be explained in two ways. First, the hydrolysis of RNA and the RNA integrity can be affected by the conditions of RNA isolation (Scheele and Hanafusa, 1972; Chen *et al.*, 1980) and virus maturation (Stoltzfus and Snyder, 1975; Štokrová *et al.*, 1982). The second explanation takes into account the heterogeneous nature of avian myeloblastosis virus (AMV-S) which was used in our experiments. It is known that the AMV acute leukaemogenic componen tin the AMV-S complex is accompanied by natural helper myeloblastosis-associated viruses, MAV-1 and MAV-2. The size of the AMV genome (4.9 megadaltons) is only slightly smaller (within 10%) than that of its natural helpers (5.3 megadaltons) (Bergmann *et al.*, 1980; Souza *et al.*, 1980) and cannot significantly affect the length distribution profiles shown. Moreover, the typical infectious AMV stock helper viruses are present in a large excess over the defective AMV (Duesberg, 1980). As it is not possible to exclude the different sensitivity of genomic RNAs of AMV and helper viruses (both present in AMV-S) to the observed splitting, the variations in the proportions of the two types of viruses could result in a different proportion of subgenomic fragments in different AMV-S preparations. A more detailed analysis of the myeloblastosis-associated virus (MAV-2) is in progress.

Acknowledgements. The authors are indebted to Dr. A. Malý for testing the proteosynthetic activity, and to Dr. A. Šulová for RNA strand separation. Skillful technical assistance of Mrs. K. Zabloudilová and Mr. P. Formánek is gratefully acknowledged.

References

Bergmann, D. G., Souza, L. M., and Baluda, M. A. (1980): Characterization of avian myeloblastosis-associated virus DNA intermediates. *J. Virol.* **34**, 366–372.

Cavalieri, L. F. (1974): Extent of doublestrandedness in avian myeloblastosis virus RNA. *J. Virol.* **14**, 1458–1462.

Chen, M. J., Garon, C. F., and Papas, T. S. (1980): Native ribonucleoprotein is an efficient transcriptional complex of avian myeloblastosis virus. *Proc. natn. Acad. Sci. U.S.A.* **77**, 1296–1300.

Chi, Y. Y., and Bassel, A. R. (1975): Electron microscopy of viral RNA: avian tumor virus RNA. *Virology* **64**, 217—227.

Davis, R. W., Simon, M. N., Davidson, N. (1971): Electron microscope heteroduplex methods for mapping regions of base sequence homology in nucleic acids, pp. 413—438. In L. Grossman, and K. Moldave (Eds.): *Methods in Enzymology* **21D**, Academic Press, New York.

Duesberg, P. H. (1968): Physical properties of Rous sarcoma virus RNA. *Proc. natn. Acad. Sci. U.S.A.* **60**, 1511—1518.

Duesberg, P. H., Bister, K., and Moscovici, C. (1980): Genetic structure of avian myeloblastosis virus released from transformed myeloblasts as a defective virus particle. *Proc. natn. Acad. Sci. U.S.A.* **77**, 5120—5124.

Erikson, R. L. (1969): Studies on the RNA from avian myeloblastosis virus. *Virology* **37**, 124—131.

Gonda, T. J., Sheiness, D. K., Fanshier, L., Bishop, J. M., Moscovici, C., and Moscovici, M. G. (1981): The genome and the intracellular RNAs of Avian Myeloblastosis Virus. *Cell* **23**, 279—290.

Hayward, W. S. (1977): Size and genetic content of viral RNAs in avian oncovirus-infected cells. *J. Virol.* **24**, 47—63.

Heine, U. I., Weber, G. H., Cottler-Fox, M., Layard, M. W., Stephenson, M. L., and Zamecnik, P. C. (1975): Analysis of oncornavirus RNA subunits by electron microscopy. *Proc. natn. Acad. Sci. U.S.A.* **72**, 3716—3720.

Kleinschmidt, A. K., and Zahn, R. K. (1959): Über Desoxyribonucleinsäure-Molekulen in Protein Mischfilmen. *Z. Naturforsch.* **146**, 770—779.

Korb, J., Trávníček, M., and Říman, J. (1976): The oncornavirus maturation process: Quantitative correlation between morphological changes and conversion of genomic virion RNA. *Intervirology* **7**, 211—224.

Korb, J., Heine, U. (1978): Size and secondary structure of avian myeloblastosis virus associated ribosomal RNA: Comparison with cellular and precursor ribosomal RNA. *Arch. Virol.* **56**, 211—225.

Korb, J., Štokrová, J., and Heine, U. I. (1981): Linear density of nucleic acid molecules as a function of denaturing and spreading conditions in electron microscopic analysis. *Studia biophys.* **84** (3), 195—206.

Kung, H.-J., Bailey, J. M., Davidson, N., Nicolson, M. O., and McAllister, R. M. (1975): Structure, subunit composition and molecular weight of RD-114 RNA. *J. Virol.* **16**, 397—411.

Malý, A., Šulová, A., Trávníček, M., Dvořák, M., and Říman, J. (1980): Translation of genomic avian myeloblastosis virus RNA in cell-free protein synthesis system for rabbit reticulocytes. *Acta virol.* **24**, 1—11.

Robberson, D., Aloni, Y., Attardi, G., and Davidson, N. (1971): Expression of the mitochondrial genome in HeLa cells. VI. Size determination of mitochondrial ribosomal RNA by electron microscopy. *J. molec. Biol.* **60**, 473—484.

Říman, J., and Beaudreau, G. S. (1970): Viral DNA-dependent DNA polymerase and the properties of thymidine labelled material in virions on an oncogenic RNA virus. *Nature (Lond.)* **228**, 427—430.

Scheele, Ch. M., and Hanafusa, H. (1972): Electrophoretic analysis of the RNA of avian tumor viruses. *Virology* **50**, 753—764.

Spector, D. H., Baker, B., Varmus, H. E., and Bishop, J. M. (1978): Characteristics of cellular RNA related to the transforming gene of avian sarcoma viruses. *Cell* **13**, 381—386.

Spiegelman, S., Burny, A., Das, M. S., Schlom, J., Trávníček, M., and Watson, K. (1970): Characterization of the products of RNA-directed DNA polymerase in oncogenic RNA viruses. *Nature (Lond.)* **227**, 663—567.

Spirin, A. S. (1963): Some problems concerning macromolecular structure of ribonucleic acids, pp. 301—345. In J. N. Davidson and W. E. Cohn (Eds): *Progress in Nucleic Acid Research*, Vol. I, Academic Press, New York.

Souza, L. M., Komaromy, M. C., and Baluda, M. A. (1980): Identification of a proviral genome associated with avian myeloblastosis leukemia. *Proc. natn. Acad. Sci. U.S.A.* **77**, 3004—3008.

Stoltzfus, C. M., and Snyder, P. N. (1975): Structure of B77 sarcoma virus RNA: Stabilization of RNA after packing. *J. Virol.* **16**, 1161—1170.

Štokrová, J., and Korb, J. (1977): Studies on the subunit structure of the genomic RNA from RNA oncogenic virus, pp. 351—352. In V. Viklický and J. Ludvík (Eds): *Proceedings of the 15th Conference on Electron Microscopy* (Prague).

Štokrová, J., Korb, J., and Říman, J. (1982): Studies on the structure of RNA from Avian Myeloblastosis Virus (AMV). II. Integrity of the RNA in the dependence on RNA isolation and virus propagation. *Acta virol.* **26**, 12–24.

Trávníček, M., and Říman, J. (1966): Evidence of nuclease activities associated with the preparations of virus BAI strain A. *Neoplasma* **13**, 377–384.

Trávníček, M., and Říman, J. (1973): Subunits of oncornavirus high-molecular-weight RNA. I. Stepwise conversion of 60S AMV (avian myeloblastosis virus) RNA to subunits. *Biochem. biophys. Res. Commun.* **53**, 217–223.

Explanation of Electron Micrographs (Plates XXXVI–XXXVII):

Fig. 1. Electron microscopic visualization of 35S AMV RNA under strongly denaturing conditions (78% formamide — 3.9 mol/l urea, 53 °C). The bar represents 0.2 µm.

Fig. 4. Electron micrographs of 35S AMV RNA fragments separated in the denaturing sucrose gradient (0.1 mol/l glyoxal).

The peak fractions were examined in the electron microscope.

The bar represents 0.2 µm.

I — fraction sedimenting at 32S
II — fraction sedimenting at 28S
III — fraction sedimenting at 24S
IV — fraction sedimenting at 18S